

# Elimination of Spurious Loss in Euler Equation Computations

Mark Drela,\* Ali Merchant,† and Jaime Peraire‡

Massachusetts Institute of Technology, Cambridge, Massachusetts 02139

The accuracy of a standard implicit conservative Euler equation solver is greatly improved by incorporation of an entropy-conservation equation, used in lieu of the streamwise momentum equation in all regions of the flow except at shock waves. A slight modification is also required at stagnation points to maintain a well-posed nature. The overall method eliminates spurious entropy errors and, thus, reduces the grid density required to achieve any particular level of accuracy. Results are presented for subsonic and transonic airfoil flows. Although the derivation and results are for steady, two-dimensional Euler equations, the approach has no inherent limitations that preclude extension to unsteady, three-dimensional, or viscous flows. A brief discussion of these extensions is presented.

## Nomenclature

$c$	= speed of sound
$D/Dt$	= substantial derivative ( $\partial/\partial t + \mathbf{q} \cdot \nabla$ )
$E$	= total energy
$f$	= momentum-conservation trigger
$g$	= stagnation trigger
$H$	= total enthalpy
$h$	= static enthalpy
$\ell$	= cell size
$M$	= Mach number
$p$	= pressure
$Q$	= enthalpy flux
$q$	= speed, $ \mathbf{q} $
$\mathbf{q}$	= velocity vector
$R$	= residual
$S$	= entropy
$t$	= time
$u, v$	= velocity components
$\alpha$	= angle of attack
$\gamma$	= specific-heat ratio
$\delta(\ )$	= upwinding change
$\varepsilon$	= viscous dissipation
$\lambda$	= characteristic speed
$\rho$	= mass density
$\bar{\tau}$	= shear stress tensor

## I. Introduction

**M**OST current Euler equation solution methods solve the mass, momentum, and energy equations discretized in strongly conservative form:

$$\frac{\partial \rho}{\partial t} + \nabla \cdot (\rho \mathbf{q}) = 0 \quad (1)$$

$$\frac{\partial (\rho u)}{\partial t} + \nabla \cdot (\rho q u + p \hat{i}) = 0 \quad (2)$$

$$\frac{\partial (\rho v)}{\partial t} + \nabla \cdot (\rho q v + p \hat{j}) = 0 \quad (3)$$

$$\frac{\partial (\rho E)}{\partial t} + \nabla \cdot (\rho q H) = 0 \quad (4)$$

The velocity vector  $\mathbf{q}$  and its magnitude  $q$  are defined in terms of the Cartesian velocity components

$$\mathbf{q} = u\hat{i} + v\hat{j}, \quad q^2 = u^2 + v^2$$

where the flow variables are defined as usual:

$$p = (\gamma - 1)(\rho E - \frac{1}{2}\rho q^2), \quad H = E + p/\rho = h + \frac{1}{2}q^2$$

$$c^2 = \gamma p/\rho, \quad M = q/c$$

The mass, momentum, and energy equations can be combined to yield the entropy conservation equation

$$\frac{\partial (\rho S)}{\partial t} + \nabla \cdot (\rho q S) = 0 \quad (5)$$

where

$$S \equiv \ell \ln(h^{1/(\gamma-1)}/p) \quad (6)$$

which shows that the entropy  $S$  should be constant throughout the flow if it is constant at the upstream boundary. In practice, however, the discrete forms of Eqs. (1–4) must be stabilized with dissipative terms, which either appear naturally as truncation errors or are added explicitly, depending on the discretization scheme used. With the additional dissipative terms, Eq. (5) will now have a positive source term on the right-hand side, giving entropy generation along streamlines. This loss production is correct only at shocks, where the dissipative terms give losses that are consistent with the proper Rankine–Hugoniot jumps. Away from shocks, however, the additional terms produce spurious losses that degrade solution accuracy.

The entropy-conservation equation (5) is used to replace the streamwise momentum equation in the viscous/inviscid MSES Euler code<sup>1</sup> in all regions of the flow except at shocks. Spurious losses are thus eliminated, allowing acceptable solutions on extremely coarse grids. Other loss-mitigation techniques have been presented by Lee and Chu,<sup>2</sup> who employ a Clebsch velocity decomposition, and by Denton and Xu,<sup>3</sup> who employ the entropy conservation equation with an ad hoc source term at shocks. More recently, Hafez and Guo<sup>4</sup> have presented a formulation using a relaxation scheme of the Cauchy/Riemann equations for the velocity components that have the total enthalpy and the entropy in their source terms. The entropy is updated by solving an entropy convection equation downstream of shocks. The total enthalpy is assumed constant, although its convection equation could easily be employed instead.

All of these previous approaches have assumed a particular topology of the flow or have been restricted to special types of solution schemes. The MSES code<sup>1</sup> is strictly for steady, two-dimensional flows, using a streamline grid and a very restricted form of dissipation not suitable for more general fixed-grid solvers or for three dimensions. The scheme of Lee and Chu<sup>2</sup> uses streamline tracing

Presented as Paper 98-2424 at the AIAA 29th Fluid Dynamics Conference, Albuquerque, NM, 15–18 June 1998; received 30 June 1998; revision received 10 June 1999; accepted for publication 12 August 1999. Copyright © 1999 by the American Institute of Aeronautics and Astronautics, Inc. All rights reserved.

\*Associate Professor, Department of Aeronautics and Astronautics, MIT Room 37-475. Associate Fellow AIAA.

†Research Assistant, Department of Aeronautics and Astronautics.

‡Professor, Department of Aeronautics and Astronautics. Associate Fellow AIAA.

to solve the convection equations, loosely coupled to an iterative scheme for the Clebsch velocity potential. Denton and Xu<sup>3</sup> report poor stability near  $M = 0$  and do not show any solutions with well-resolved stagnation points. It is not clear that their scheme is consistent. The method of Hafez and Guo<sup>4</sup> requires knowledge of the location and orientation of shocks to produce the appropriate entropy sources for the entropy convection equation. This can lead to difficulties at intersecting shocks, especially in three dimensions. The singular nature of the Cauchy/Riemann equations at stagnation points is not addressed.

The remainder of this paper will focus on the formulation of an entropy-conserving method for general two- or three-dimensional Euler solvers using unstructured grids. The assumptions of steady flow or constant total enthalpy will not be required. Only the approximate location of shocks will be required; knowledge of shock orientation will not be necessary. The issue of consistency, and a well-posed nature at stagnation points will be addressed in considerable detail. Results for subsonic and transonic two-dimensional Euler flows will be presented. Extensions to three-dimensional and Navier-Stokes solvers will also be discussed.

## II. Discrete Formulation and Artificial Dissipation

A fairly general way to describe upwinded conservative schemes is to include a dissipative upwinding change to each flux component:

$$\frac{\partial \rho}{\partial t} + \nabla \cdot [\rho \mathbf{q} - \lambda \delta \rho] = 0 \quad (7)$$

$$\frac{\partial(\rho u)}{\partial t} + \nabla \cdot [\rho q u + p \hat{t} - \lambda \delta(\rho u)] = 0 \quad (8)$$

$$\frac{\partial(\rho v)}{\partial t} + \nabla \cdot [\rho q v + p \hat{j} - \lambda \delta(\rho v)] = 0 \quad (9)$$

$$\frac{\partial(\rho E)}{\partial t} + \nabla \cdot [\rho q H - \lambda \delta(\rho E)] = 0 \quad (10)$$

The notation  $\delta f$  denotes a change in  $f$  in some direction, proportional either to  $\ell$  for first-order dissipation or to  $\ell^3$  for third-order dissipation,  $\ell$  being the cell size. The weight  $\lambda$  is a small coefficient that can take different forms in different upwinding methods and can also be a matrix to give the characteristic-based or matrix-dissipation methods. These distinctions are not important here.

The additional dissipation terms produce streamwise changes in the entropy that would otherwise be constant barring truncation errors. The associated entropy source terms can be determined by deriving an expression for the material derivative of the entropy, whose form follows from definition (6):

$$\begin{aligned} dS &= \frac{\gamma}{\gamma - 1} \frac{dh}{h} - \frac{dp}{p}, & p dS &= \rho dH - \rho q dq - dp \\ p \frac{DS}{Dt} &= \rho \frac{DH}{Dt} - \rho q \frac{Dq}{Dt} - \frac{Dp}{Dt} \end{aligned} \quad (11)$$

The right-hand-side terms of Eq. (11) are determined from the modified momentum and energy equations (8–10) by first expanding these as

$$\begin{aligned} \frac{\partial(\rho u)}{\partial t} + u \nabla \cdot [\rho \mathbf{q} - \lambda \delta \rho] + \rho \mathbf{q} \cdot \nabla u + \frac{\partial p}{\partial x} \\ &= \nabla \cdot [\lambda \delta(\rho u)] - u \nabla \cdot [\lambda \delta \rho] \\ \frac{\partial(\rho v)}{\partial t} + v \nabla \cdot [\rho \mathbf{q} - \lambda \delta \rho] + \rho \mathbf{q} \cdot \nabla v + \frac{\partial p}{\partial y} \\ &= \nabla \cdot [\lambda \delta(\rho v)] - v \nabla \cdot [\lambda \delta \rho] \\ \frac{\partial(\rho H)}{\partial t} + H \nabla \cdot [\rho \mathbf{q} - \lambda \delta \rho] + \rho \mathbf{q} \cdot \nabla H - \frac{\partial p}{\partial t} \\ &= \nabla \cdot [\lambda \delta(\rho E)] - H \nabla \cdot [\lambda \delta \rho] \end{aligned}$$

from which follow their corresponding modified convective forms using the modified mass equation:

$$\begin{aligned} \rho \frac{Du}{Dt} + \frac{\partial p}{\partial x} &= \nabla \cdot [\lambda \delta(\rho u)] - u \nabla \cdot [\lambda \delta \rho] \\ &= \nabla \cdot [\lambda \rho \delta u] + \nabla u \cdot \lambda \delta \rho \end{aligned} \quad (12)$$

$$\begin{aligned} \rho \frac{Dv}{Dt} + \frac{\partial p}{\partial y} &= \nabla \cdot [\lambda \delta(\rho v)] - v \nabla \cdot [\lambda \delta \rho] \\ &= \nabla \cdot [\lambda \rho \delta v] + \nabla v \cdot \lambda \delta \rho \end{aligned} \quad (13)$$

$$\begin{aligned} \rho \frac{DH}{Dt} - \frac{\partial p}{\partial t} &= \nabla \cdot [\lambda \delta(\rho E)] - H \nabla \cdot [\lambda \delta \rho] \\ &= \nabla \cdot [\lambda \rho \delta H] + \nabla H \cdot \lambda \delta \rho - \nabla \cdot [\lambda \delta p] \end{aligned} \quad (14)$$

Combining Eq. (14) –  $u$ [Eq. (12)] –  $v$ [Eq. (13)] produces the desired expression for the convective rate of change of entropy:

$$\begin{aligned} \rho \frac{DH}{Dt} - \rho q \frac{Dq}{Dt} - \frac{Dp}{Dt} &= \nabla \cdot [\lambda(\rho \delta h - \delta p)] + \nabla h \cdot \lambda \delta \rho \\ &+ \nabla u \cdot \lambda \rho \delta u + \nabla v \cdot \lambda \rho \delta v \end{aligned} \quad (15)$$

$$\rho \frac{DS}{Dt} = \nabla \cdot [\lambda \rho \delta S] + \nabla H \cdot \lambda \delta \rho + \rho^2 \left( \nabla u \cdot \lambda \delta \left( \frac{u}{\rho} \right) + \nabla v \cdot \lambda \delta \left( \frac{v}{\rho} \right) \right) \quad (16)$$

The first term on the right-hand side of Eq. (16) is simply a diffusion term. The second term is responsible for entropy production in a shock moving through stationary fluid, whereas the third term is responsible for entropy production in a stationary shock (where  $H$  is constant and the second term disappears). For first-order, gradient-based dissipation,  $\nabla u$  and  $\delta u$  are parallel vectors, and so the third term is clearly positive definite. For the moving shock, the rise in  $H$  (or  $h$ ) is caused by volumetric compression work associated with the change in  $\rho$ , so that  $\nabla H$  and  $\delta \rho$  are essentially parallel, making the second term positive definite as well. The net result is that entropy in a numerical solution using gradient-based dissipation increases monotonically downstream, aside from the possibility of lateral diffusion from an adjacent lower-entropy region.

It is useful to examine the effect of using the total enthalpy rather than the total energy to form the dissipation term in the modified energy equation (10), as suggested by Jameson et al.<sup>5</sup>:

$$\frac{\partial(\rho E)}{\partial t} + \nabla \cdot [\rho q H - \lambda \delta(\rho H)] = 0 \quad (17)$$

This has the advantage of giving perfectly constant  $H$  in a steady solution. The entropy transport equation now becomes the following:

$$\rho \frac{DS}{Dt} = \nabla \cdot [\lambda \rho \delta h] + \nabla H \cdot \lambda \delta \rho + \rho^2 \left( \nabla u \cdot \lambda \delta \left( \frac{u}{\rho} \right) + \nabla v \cdot \lambda \delta \left( \frac{v}{\rho} \right) \right) \quad (18)$$

The first term on the right-hand side is no longer strictly diffusive in the presence of varying pressure gradients, producing nonmonotonic entropy evolution along streamlines. This lack of a proper diffusion term also makes the entropy perturbation mode poorly damped, which is consistent with the observation that this form of dissipation is somewhat less stable.

## III. Entropy-Conserving Formulation

The approach taken here is to effectively solve the entropy conservation equation (5) in lieu of some combination of the standard mass, momentum, and energy equations. Like the standard equations, the entropy equation must also be stabilized with added dissipation (which is not dissipative in the thermodynamic sense). A suitable form is

$$\frac{\partial(\rho S)}{\partial t} + \nabla \cdot [\rho q S - \lambda \delta(\rho S)] = 0 \quad (19)$$

which, if employed together with the upwinded mass equation (7), will produce perfectly constant entropy in steady state despite the upwinding.

It is convenient to define shorthand for the residuals appearing in all of the conservation equations:

$$\begin{aligned} R_\rho &\equiv \nabla \cdot [\rho \mathbf{q} - \lambda \delta \rho], & R_u &\equiv \nabla \cdot [\rho q u + p \hat{i} - \lambda \delta(\rho u)] \\ R_v &\equiv \nabla \cdot [\rho q v + p \hat{j} - \lambda \delta(\rho v)], & R_H &\equiv \nabla \cdot [\rho q H - \lambda \delta(\rho H)] \\ R_S &\equiv \nabla \cdot [\rho q S - \lambda \delta(\rho S)] \end{aligned}$$

The formulation will make use of the following convective residuals:

$$\begin{aligned} R'_u &\equiv R_u - u R_\rho, & R'_v &\equiv R_v - v R_\rho \\ R'_H &\equiv R_H - H R_\rho, & R'_S &\equiv R_S - S R_\rho \end{aligned}$$

These are still discretized in strongly conservative form as shown, to allow correct shock capturing. It is also convenient to define the convective streamwise and normal momentum residuals:

$$R'_q = (u/q) R'_u + (v/q) R'_v, \quad R'_n = -(v/q) R'_u + (u/q) R'_v$$

It is readily verified that the following combination is a higher-order quantity:

$$R_\epsilon \equiv R'_H - q R'_q - (p/\rho) R'_S = \mathcal{O}(|\delta|) \quad (20)$$

This simply reflects that  $S$  is not an independent variable, so that  $R'_S$  must be expressible in terms of the other residuals to within truncation error. With the present gradient-based dissipation,  $R_\epsilon$  has the following form to leading order:

$$R_\epsilon = -\nabla \cdot [\lambda \delta p] - (1/\rho) \nabla p \cdot (\lambda \delta \rho) - \nabla u \cdot (\lambda \rho \delta u) - \nabla v \cdot (\lambda \rho \delta v) \quad (21)$$

Because  $R_\epsilon$  is a higher-order quantity, it is legitimate to set  $R_\epsilon = 0$  in relation (20):

$$R'_H - q R'_q - (p/\rho) R'_S = 0$$

and then use this relation to replace any one of these three residuals with the remaining two. This is equivalent to adding an appropriate multiple of the dissipation or truncation-error terms, so that this modification will preserve consistency. The key idea behind the present scheme is to use the best combination of residuals at every point in the flowfield to maximize accuracy of the discrete solution.

Most of the inaccuracies of conventional Euler solvers are due to their spurious entropy layers that typically form adjacent to surfaces. In the presence of pressure gradients, these layers have displacement effects on the outer potential flow, with the attendant loss of lift, nonzero pressure drag, etc. As shown in the preceding section, this spurious entropy production in standard Euler schemes is inevitable and is arguably their worst feature. Because  $R'_S = 0$  implies constant entropy, and  $R'_H = 0$  is already being solved, all such spurious entropy production can be eliminated by making the substitution

$$q R'_q \rightarrow R'_H - (p/\rho) R'_S \quad (22)$$

which discards momentum conservation in favor of entropy conservation. One can consider the switch in equations to be equivalent to adding streamwise momentum sources such that all entropy variations are suppressed. Relation (20) indicates that the change has no effect to within the dissipation or truncation error, that is, the sources are of higher order, so that consistency is unaffected. It is asserted that conserving entropy is preferable in all situations except at shocks, where momentum must be conserved to obtain the correct Rankine-Hugoniot shock jumps.

The substitution (22) is not usable directly because at a stagnation point where  $q = 0$  the entropy is stationary with respect to  $q$  (it depends on  $q^2$ ). Hence, the entropy is not influenced by momentum sources at a stagnation point, so that constant entropy cannot be enforced simply by modifying  $R'_q$  in this manner. A singular equation system is produced if this is attempted. The following formulation combines all of the equations in a manner that precludes such singularities.

The steady-state equation system for the momentum-conserving case is expressed in vector form as follows:

$$\mathbf{R}_m \equiv \begin{Bmatrix} c R_\rho \\ R'_u \\ R'_v \\ R'_H \end{Bmatrix} = \mathbf{0} \quad (23)$$

This will permit correct shock capturing provided the convective residuals are discretized in strongly conservative form as discussed earlier. The equation switching to the alternative entropy-conserving form is conveniently performed with the unit vector

$$\hat{\mathbf{r}} = \left\{ \frac{g}{G}, \frac{1-g}{G} \frac{u}{q}, \frac{1-g}{G} \frac{v}{q}, 0 \right\}^T, \quad G = \sqrt{1 - 2g + 2g^2} \quad (24)$$

where  $g$  is a heuristic switch that is 1 near stagnation points and 0 everywhere else:

$$g = \exp[-(M/0.05)^2] \quad (25)$$

An isentropic (entropy-conserving) residual vector is now defined as

$$\mathbf{R}_{is} \equiv \mathbf{R}_m - \hat{\mathbf{r}} [\hat{\mathbf{r}} \cdot \mathbf{R}_m + A(c/\gamma) R'_S] \quad (26)$$

$$A = [(1-g)/G](c/q) + g/G \quad (27)$$

where the weighting factor  $A$  merely serves to make the system better-conditioned numerically as  $q \rightarrow 0$  and  $g \rightarrow 1$  near a stagnation point. Note that

$$\hat{\mathbf{r}} \cdot \mathbf{R}_{is} = -A(c/\gamma) R'_S \quad (28)$$

and  $A$  is never zero, so that enforcing  $\mathbf{R}_{is} = \mathbf{0}$  will force  $R'_S = 0$  and produce perfectly isentropic flow.

#### IV. Hybrid Method for Shocks

The momentum-conserving and entropy-conserving residual vectors are now combined into a net residual vector:

$$\mathbf{R} \equiv f \mathbf{R}_m + (1-f) \mathbf{R}_{is} = \mathbf{0}$$

where  $f$  is a locally defined momentum-conservation trigger. If  $f = 1$ , then the standard momentum-conserving scheme is recovered. If  $f = 0$ , then entropy is conserved in lieu of streamwise momentum (or in lieu of mass conservation at stagnation points). A more explicit expression for the net residual vector  $\mathbf{R}$  to be solved is as follows:

$$\mathbf{R} = \mathbf{R}_m - (1-f) \hat{\mathbf{r}} \{ (g/G) c R_\rho + [(1-g)/G] R'_q + A(c/\gamma) R'_S \} \quad (29)$$

It is necessary to examine the consistency and well-posed nature of  $\mathbf{R}$  for intermediate values of  $f$  as well as  $g$ . This is done by using the following orthogonal basis:

$$\bar{\mathbf{T}} \equiv \begin{bmatrix} (1-g) & -g(u/q) & -g(v/q) & 0 \\ g & (1-g)(u/q) & (1-g)(v/q) & 0 \\ 0 & -v/q & u/q & 0 \\ 0 & 0 & 0 & 1 \end{bmatrix}$$

Note that  $\bar{\mathbf{T}} \hat{\mathbf{r}} = \{0 \ G \ 0 \ 0\}^T$ . Two cases are now considered.

1) Near a shock,  $g = 0$  and  $f$  arbitrary,

$$\begin{bmatrix} 1 & 0 & 0 & 0 \\ 0 & q & 0 & 1-f \\ 0 & 0 & 1 & 0 \\ 0 & 0 & 0 & 1 \end{bmatrix} \bar{\mathbf{T}} \mathbf{R} = \begin{Bmatrix} c R_\rho \\ q R'_q + (1-f) R_\epsilon \\ R'_n \\ R'_H \end{Bmatrix}$$

$$\begin{bmatrix} 1 & 0 & 0 & 0 \\ 0 & q & 0 & -f \\ 0 & 0 & 1 & 0 \\ 0 & 0 & 0 & 1 \end{bmatrix} \bar{\mathbf{T}} \mathbf{R} = \begin{Bmatrix} c R_\rho \\ -(p/\rho) R'_S - f R_\epsilon \\ R'_n \\ R'_H \end{Bmatrix}$$

The first form confirms that the method conserves momentum for  $f = 1$ , and the second confirms that it conserves entropy for  $f = 0$ . Both forms also show that the method remains consistent for any intermediate value of  $f$  because it multiplies  $R_\epsilon$ , which is a higher-order quantity.

2) Near stagnation,  $f = 0$  and  $g$  arbitrary,

$$\begin{bmatrix} q & gc/GA & 0 & g \\ 0 & 1 & 0 & 0 \\ 0 & 0 & 1 & 0 \\ 0 & 0 & 0 & 1 \end{bmatrix} \bar{\mathbf{T}}\mathbf{R}_{\text{is}} = \begin{bmatrix} (1-g)qcR_p + gR_\epsilon \\ -GA(c/\gamma)R'_s \\ R'_n \\ R'_H \end{bmatrix}$$

Here, the effect of varying  $g = 0 \rightarrow 1$  is to gradually replace the continuity residual  $R_p$  with  $R_\epsilon$ . Again, the system remains consistent for any value of  $g$ , except possibly in the limiting case  $g = 1$ , where  $R_\epsilon$  alone remains. As can be seen from its expansion (21), the leading term of  $R_\epsilon$  is

$$R_\epsilon = -\nabla \cdot [\lambda \delta p] + \dots$$

which mimics  $\nabla^2 p$  for first-order dissipation and  $\nabla^4 p$  for third-order dissipation. In either case,  $R_\epsilon$  is in effect a regularity constraint on the pressure and, hence, plays the same role as the continuity equation that it replaces. The discrete system, therefore, remains well posed even for the limiting case  $g = 1$ , as confirmed by the computed results. This substitution does, of course, incur mass-conservation errors near the stagnation point, but these occur over an area that is  $\mathcal{O}(\ell^2)$  (essentially one cell) as can be seen from  $g$  definition (25).

A suitable expression for the momentum conservation trigger (a shock finder, ideally) is based on the undivided convective rate of change of density in the cell:

$$\mathcal{D}_f = (\ell/\rho c) \mathbf{q} \cdot \nabla \rho$$

$$f = \begin{cases} 1 - \exp[-(1000 \mathcal{D}_f)^2], & \mathcal{D}_f > 0 \\ 0, & \mathcal{D}_f < 0 \end{cases} \quad (30)$$

Note that an expansion has  $\mathcal{D}_f < 0$  and remains isentropic. For unsteady flows, frame-invariant definitions such as

$$\mathcal{D}_f = \frac{\ell}{\rho c} \frac{D\rho}{Dt} \quad \text{or} \quad \mathcal{D}_f = \frac{\ell}{pc} \frac{Dp}{Dt}$$

would be preferable to Eq. (30). This is a minor distinction.

## V. Solution Method

The solution technique employed here is Newton's method applied directly to the steady residuals (29). At each Newton iteration, the linearized system is solved and the state vector  $\mathbf{U}$  is updated:

$$\left( \frac{\partial \mathbf{R}}{\partial \mathbf{U}} \right) \delta \mathbf{U} = -\mathbf{R}, \quad \mathbf{U} \leftarrow \mathbf{U} + \delta \mathbf{U}$$

The linear system is solved with GMRES,<sup>6</sup> using a sparse incomplete LU-factorization solver, created by Y. Saad [SPARSKIT, a basic tool kit for sparse matrix computations, user guide, and documentation, 1990 (unpublished)], as a preconditioner.

The combined net residual  $\mathbf{R}$ , together with the entropy definition (6) fully determines the time rate of change of the standard conservative-scheme state vector:

$$\frac{\partial}{\partial t} \{\rho \quad \rho u \quad \rho v \quad \rho E\}^T$$

for any value of  $f$  and  $g$  and can, therefore, in principle be used with any standard explicit time-marching scheme. Unfortunately, all such explicit schemes have been found to become unstable when entropy is conserved (when  $f = 0$ ). This is perhaps not too surprising because the residual contributions effectively added to conserve entropy must be antidissipative to offset the natural dissipation of the momentum-conserving scheme. The fully implicit direct Newton solver used here remains stable with this added negative dissipation.

**Table 1 Test cases**

Case	$\alpha$ , deg	$M_\infty$	Surface points	Major features
1a, 1b	9	0.30	28, 42, 70, 112	Leading-edge suction peak
2a, 2b	3	0.80	90	Upper-side shock

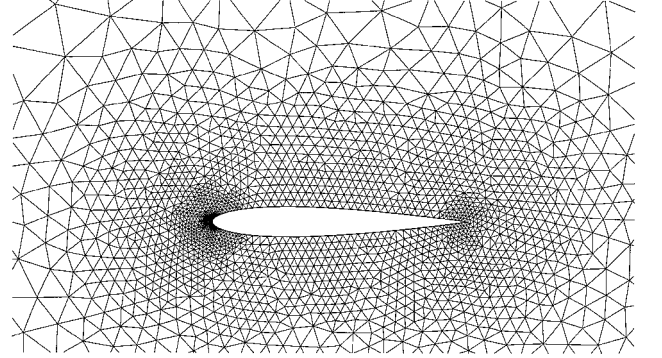


**Fig. 1 Grid near NACA 0012 airfoil.**

## VI. Results

The present scheme was implemented in an unstructured-grid, two-dimensional Euler code, using grids generated by the FELISA three-dimensional grid generator.<sup>7</sup> The NACA 0012 airfoil was run using the case parameters given in Table 1. Cases 1a and 2a use the conventional momentum-conserving Euler method ( $f = 1$  everywhere), and cases 1b and 2b use the entropy-conserving formulation ( $f = 1$  at shock,  $f = 0$  elsewhere). Cases 1a and 1b were also used in a grid-dependence study with the number of grid points on the airfoil perimeter varied from 28 to 112.

Figure 1 shows the unstructured grid near the airfoil with 90 surface points. This is a moderately dense grid for two-dimensional cases, but it is representative of a section of a rather dense three-dimensional grid.

### A. Case 1: Subsonic Airfoil

Figure 2 shows the Mach and entropy contours for case 1a, computed on the 90-surface-point grid. It exhibits the typical entropy layer resulting from numerical dissipation at the strong suction peak, where in this case the local Mach number is just below unity. Figure 3 shows the same case for the entropy-conserving scheme with the same contour levels. The spurious loss is entirely eliminated in the latter case.

Figure 4 shows the surface  $C_p$  distributions for the four grid densities. In both cases the coarsest grids cannot possibly resolve the sharp leading-edge  $C_p$  spike. However, the error in the overall lift of the momentum-conserving case 1a is quite significant and is apparently due to the displacement effect of the entropy layer acting near the trailing edge. In contrast, the entropy-conserving case 1b maintains its overall lift much better. Figure 5 shows the  $C_L$  and  $C_D$  dependence on grid size for the two cases. The entropy layer also causes a very significant spurious pressure drag. Note that the drag of the entropy-conserving scheme is not monotonic with the grid density, although it is clearly more accurate than the momentum-conserving scheme for practical grid sizes.

### B. Transonic Airfoil

Figure 6 shows the Mach and entropy contours for case 2a computed with the conventional Euler method. Roughly the same grid as shown in Fig. 1 was used, except that a slightly denser grid was specified over the aft portion of the airfoil to better capture the shock. In addition to the correct entropy generated at the shock, the surface entropy layers are also present as in the fully subsonic case 1a. Figure 7 shows the result for the entropy-conserving scheme. This allows loss generation only at the shock, so that the flow upstream of the shock is strictly isentropic. Figure 8 shows contours of the trigger function  $f$ , which is nonzero only at the shock, limiting entropy generation to only that region. Once the entropy is generated at the shock itself, it convects and diffuses downstream as usual into

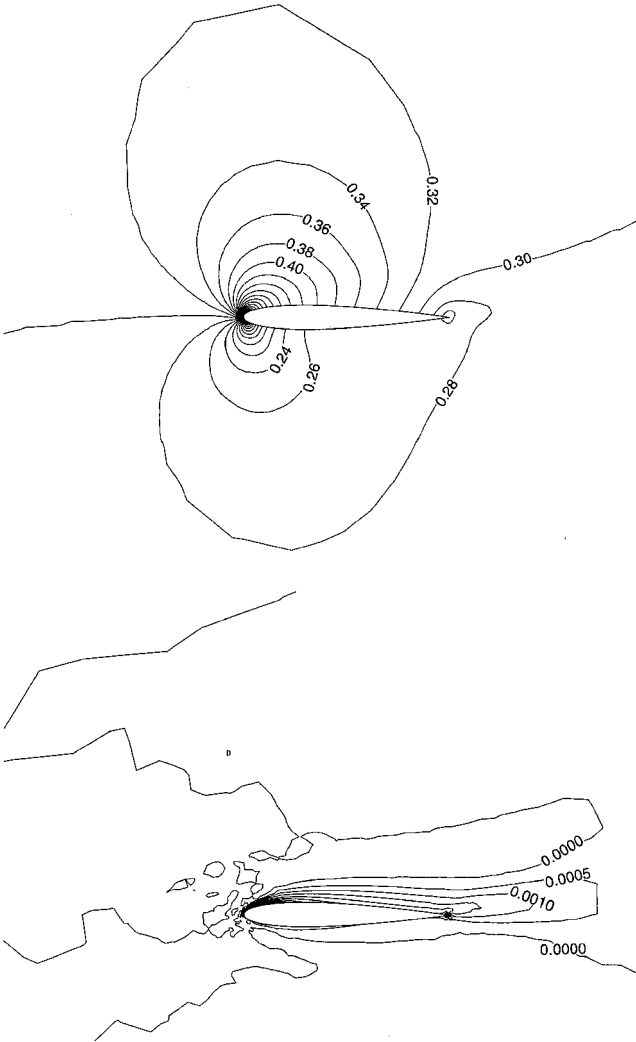


Fig. 2 Mach and entropy contours for momentum-conserving case 1a: NACA 0012 at  $\alpha = 9$  deg and  $M_\infty = 0.3$ .

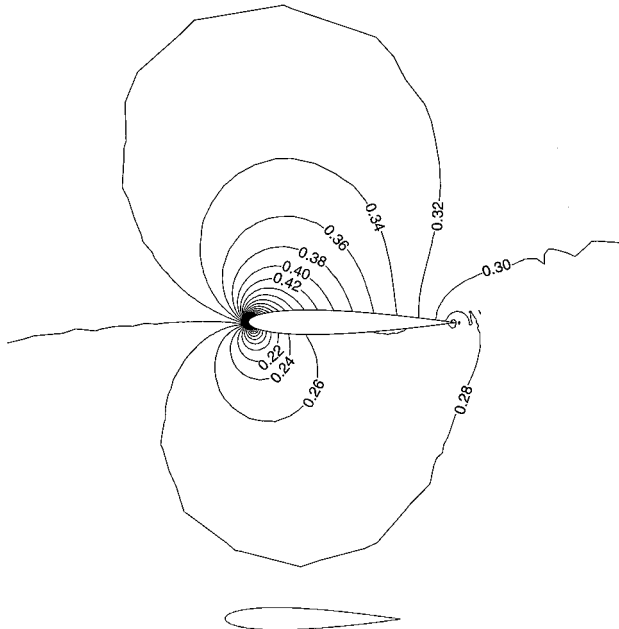


Fig. 3 Mach and entropy contours for entropy-conserving case 1b: NACA 0012 at  $\alpha = 9$  deg and  $M_\infty = 0.3$ .

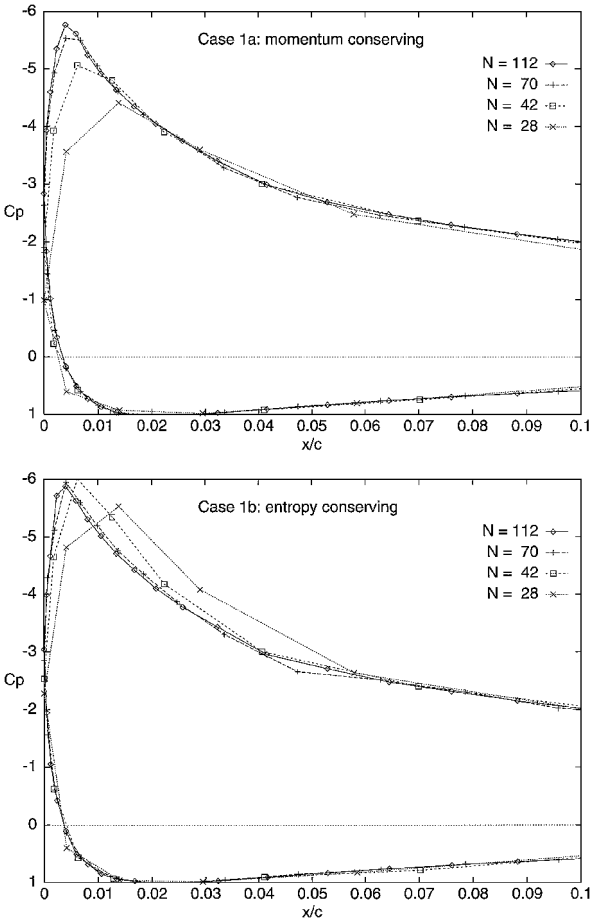


Fig. 4 Surface  $C_p$  distributions for cases 1a and 1b vs number of surface points.

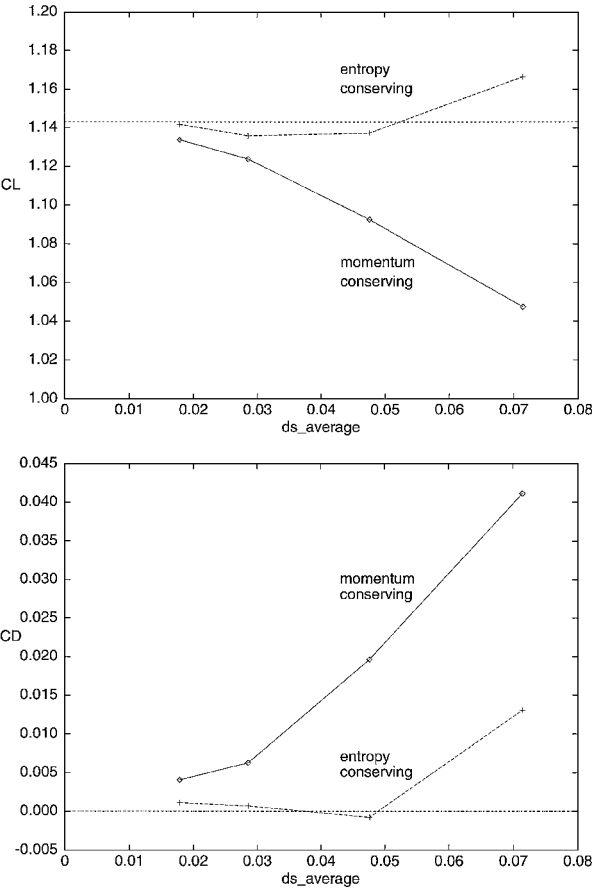


Fig. 5 Case 1  $C_L$  and  $C_D$  vs average surface cell length (chord = 1).

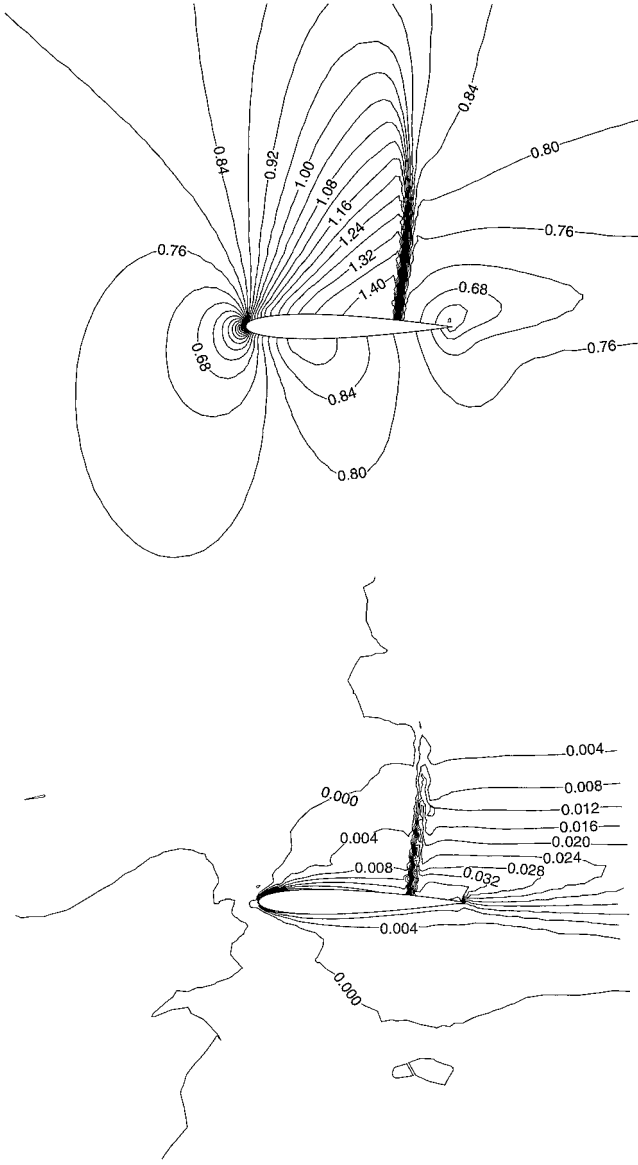


Fig. 6 Mach and entropy contours for momentum-conserving case 2a: NACA 0012 at  $\alpha = 3$  deg and  $M_\infty = 0.8$ .

the isentropic region downstream of the shock. This confirms that the present entropy-conserving scheme merely suppresses entropy production. Entropy transport is unaffected as intended.

### VII. Extensions to Viscous Flows

Current Navier–Stokes methods suffer from much the same spurious entropy production as Euler methods. For viscous flow computations on modest grids, this false entropy can be potentially even more destructive because a false entropy layer in effect adds to the momentum thickness of the real boundary layer and will change its response to pressure gradients. This can, in turn, cause substantial errors in drag and separation predictions.

The derivation of the present method does not rely on the flow being inviscid. The residual identity (20) is still valid, so that the net modified equation residual vector (29) remains consistent and the overall treatment remains essentially the same. Momentum conservation ( $f = 1$ ,  $g = 0$ ) would be appropriate at surface points where the no-slip condition enforces  $q = 0$ . The key difference is that the laminar and Reynolds-averaged shear stress tensor, heat flux, and dissipation are no longer neglected:

$$\begin{aligned}\bar{\tau} &= \mu [\nabla q + (\nabla q)^T - \frac{2}{3}(\nabla \cdot q)\bar{I}] - \rho \bar{q} \bar{q}^T \\ Q &= (\mu/Pr)\nabla h - \rho \bar{q} \bar{h}' \\ \varepsilon &= \nabla \cdot (\bar{\tau} \cdot q) - q \cdot (\nabla \cdot \bar{\tau}) = (\bar{\tau} \cdot \nabla) \cdot q\end{aligned}$$

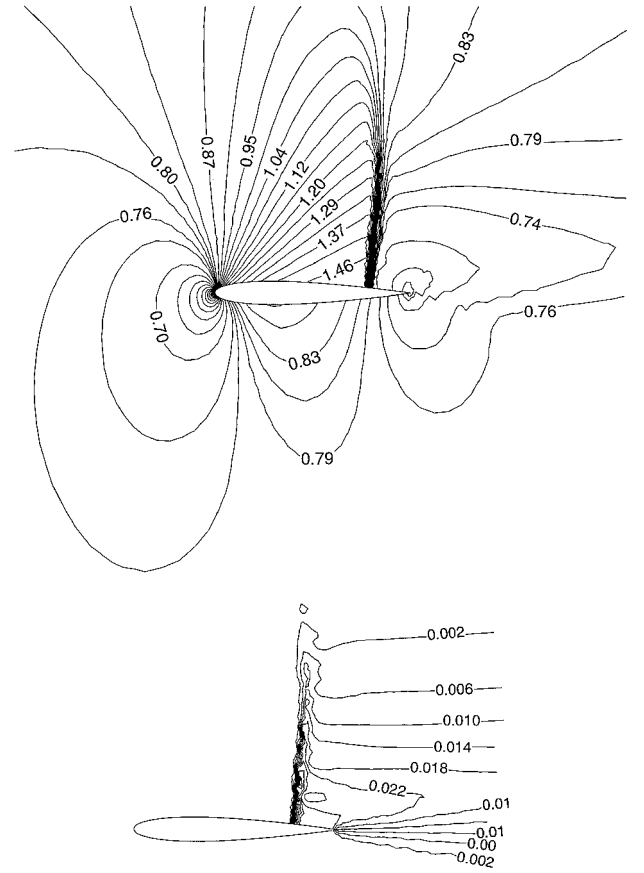
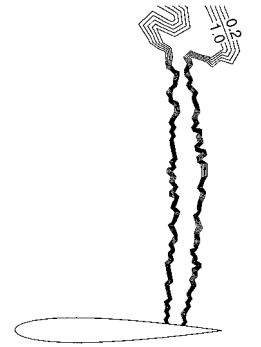


Fig. 7 Mach and entropy contours for entropy-conserving case 2b: NACA 0012 at  $\alpha = 3$  deg and  $M_\infty = 0.8$ .

Fig. 8 Contours of the trigger function  $f$  for case 2b; entropy generation occurs only where  $f > 0$  at the shock.



The momentum, energy, and entropy residuals are now defined as

$$\begin{aligned}R_u &= \nabla \cdot [\rho q u + p \hat{i} - \lambda \delta(\rho u) - \bar{\tau} \cdot \hat{i}] \\ R_v &= \nabla \cdot [\rho q v + p \hat{j} - \lambda \delta(\rho v) - \bar{\tau} \cdot \hat{j}] \\ R_H &= \nabla \cdot [\rho q H - \lambda \delta(\rho H) - \bar{\tau} \cdot q - Q] \\ R_S &= \nabla \cdot [\rho q S - \lambda \delta(\rho S)] - (\rho/p)[\varepsilon + \nabla \cdot Q]\end{aligned}$$

and  $R_S$  now has a nonzero source term as expected. Note that this source term is strictly physical and does not directly depend on the upwinding terms, and the accuracy benefits of using  $R_S$  are also expected for viscous flows away from the immediate vicinity of no-slip walls.

### VIII. Extensions to Three-Dimensional Flows

The derivation of the present method extends directly to three dimensions because only an additional  $z$ -momentum residual  $R_w$  must be introduced. One anticipated change is the likely need to extend the momentum-conservation trigger  $f$  to recognize intrinsically dissipative three-dimensional flow features beside shocks. One example is a vortex sheet with streamwise vorticity, typically

shed from a wing trailing edge. Momentum must be conserved in the sheet immediately behind the trailing edge so that the appropriate amount of entropy is generated numerically.

It is recognized that the Newton system for typical three-dimensional problems will most likely be too large to permit direct solution via elimination. It will be necessary to resort to iterative sparse-matrix solution techniques.

### IX. Conclusions

A method for eliminating spurious losses in Euler equation computations has been presented. The approach can be readily retrofitted to any implicit Euler solver with little additional computational effort and gives large improvements in accuracy on modest grids. Extensions to viscous and three-dimensional flows appear feasible.

### References

<sup>1</sup>Drela, M., "Newton Solution of Coupled Viscous/Inviscid Multielement Airfoil Flows," AIAA Paper 90-1470, June 1990.

<sup>2</sup>Lee, K. D., and Chu, S. S., "An Improvement of Convection Fidelity in Euler Calculations," AIAA Paper 89-0473, Jan. 1989.

<sup>3</sup>Denton, J. D., and Xu, L., "A New Approach to the Calculation of Transonic Flow Through Two Dimensional Turbomachine Blade Rows," American Society of Mechanical Engineers, Paper 85-GT-5, March 1985.

<sup>4</sup>Hafez, M., and Guo, W. H., "Simulation of Steady Compressible Flows Based on Cauchy/Riemann Equations and Crocco's Relation," *International Journal for Numerical Methods in Fluids*, Vol. 27, 1998, pp. 127-138.

<sup>5</sup>Jameson, A., Schmidt, W., and Turkel, E., "Numerical Solutions of the Euler Equations by Finite Volume Methods Using Runge-Kutta Time-Stepping Schemes," AIAA Paper 81-1259, June 1981.

<sup>6</sup>Saad, Y., and Schultz, M. H., "GMRES: A Generalized Minimal Residual Algorithm for Solving Nonsymmetric Linear Systems," Dept. of Computer Science, DCS Rept. RR-254, Yale Univ., New Haven, CT, Aug. 1983.

<sup>7</sup>Peraire, J., Peiro, J., and Morgan, K., "Multigrid Solution of the 3D Compressible Euler Equations on Unstructured Tetrahedral Grids," *International Journal for Numerical Methods in Engineering*, Vol. 36, 1993, pp. 1029-1044.

P. Givi  
Associate Editor